Iranian Journal of Pharmaceutical Sciences
Spring 2008: 4(2): 169-176
www.ijps.ir

Original Article

Deposition of Nano-Crystalline Fluor-hydroxyapatite Coatings on Titanium Substrates via Sol-Gel Method

Sedigheh Joughehdoust[a,*], Aliasghar Behnamghader[b], Abdollah Afshar[c]

[a]*Islamic Azad University, Science and Research Branch, Biomedical Engineering Faculty and Young Research Club, Tehran, Iran*
[b]*Material and Energy Research Center, Tehran, Iran*
[c]*Department of Material Science and Engineering, Sharif University of Technology, Tehran, Iran*

Abstract

In this investigation, fluor-hydroxyapatite (FHA) film was deposited on a titanium substrate by sol-gel method. Triethyl phosphite, ammonium fluoride and calcium nitrate in ethanol solutions were used respectively as P, F and Ca precursors. Typical apatite structures were obtained for all coatings after dipping and subsequent heat treatment at 550, 700 and 800 ºC, the coating layers were investigated with X-ray diffraction, Fourier transform infra-red and Scanning electron microscopy spectroscopy. Based on the results obtained from X-ray diffraction, the coatings heated at 550 ºC were composed of hydroxyapatite (HA) and fluorapatite (FA). Rutile (TiO_2) phase was also found in the coatings heated at higher temperature. In addition, the formation of fluor-hydroxyapatite was confirmed by FT-IR results. SEM studies showed the samples heat treated at 550 ºC and 700 ºC have almost the same morphology. It seems the coating of samples heat treated in 800 ºC was more homogenous and smooth without any considerable porosity.

Keywords: Fluor-hydroxyapatite; Rutile; Sol-gel method; Titanium substrate.
Received: December 4, 2007 *Accepted:* February 10, 2008

1. Introduction

Natural bone of human hard tissue is composed of collagen and hydroxyapatite. Hydroxyapatite (HA, $Ca_{10}(PO_4)_6(OH)_2$) bonds to bone tissue without creating fiber capsule [1]. This material is very biocompatible and has a lot of applications in the repairing of bone and tooth. The excellent biocompatibility of HA is closely related to its chemical and biological similarities with human hard tissues [2]. However, the biomaterial based on HA alone is not suitable for load bearing applications due to lower mechanical strength of HA [3, 4]. Implants of bioinert materials such as titanium, stainless steel, and titanium-vanadium alloys are used for load bearing applications. These materials are generally coated with HA or bioglass for improving the biocompatibility and tissue growth surrounding them. The detachment of the HA-based coatings due to the resorption in biological environment has been also reported [5].

*Corresponding author: Sedigheh Joughehdoust, Islamic Azad University, Science and Research Branch, Biomedical engineering Faculty, Tehran, Iran
Tel (+98)21-44474321-4, Fax (+98)21-44474319
E-mail: joughehdoust@sr.iau.ac.ir

The solubility of apatite films, which determines their longevity, is strongly influenced by both the chemical composition and the crystallinity of the apatite [6]. Pure fluorapatite (FA: $Ca_{10}(PO_4)_6F_2$) is known to have a much lower solubility than HA, because FA possesses a greater stability than HA, both chemically and structurally [7, 8]. One solution for reducting the solubility of HA coatings is replacing F^- with OH^- in HA structure, and forming fluor-hydroxyapatite [FHA, $Ca_{10}(PO_4)_6(OH,F)_2$] solid solution [9, 10]. FHA and FA crystals have been identified in bone tissue and dental enamel, respectively [11].

In practice, the fluorine ion, itself, has been studied widely in dental restoration areas, due to its advantages over other ions concerning the prevention of cavies in bacteria-existing environments [8, 12]. Also, F^- improves the mineralization and crystallization of calcium phosphate compounds during the new bone formation [13, 14]. Pure FA has a lower ability of the resorption due to their more structural compaction compared to HA [15]. We think the bioactivity of this material might be adjusted by controlling the amount of F^- in HA structure.

There are a lot of methods to prepare the HA and FA coatings on metal substrate. Currently, most HA and FA coatings are obtained using a plasma-spraying method [16, 17]. However, there are some problems associated with the plasma-spraying process, such as the poor adherence of coating to substrate and the presence of uncontrolled porosities. The formation of these defects is attributed to high temperature used in this process and very rapid cooling of coated materials [18]. In comparison, the sol-gel method has a lot of advantages in the formation of thin and compact films. The thin films prepared via sol-gel process has high chemical homogeneity, very fine structure and low crystallization temperature of the resultant coating. Recently, deposition of different calcium phosphate compounds on metallic substrates via sol-gel process has attracted much attention in the field of biomedical applications and researches [19-21]. However, there are a few reports on the deposition and characterization of sol-gel derived FHA films [5, 9, 15]. The aim of this work was to prepare FHA films via sol-gel method and to characterize its phase and morphologicl aspects.

2. Materials and methods

To deposite FHA, on the substrates, the precursors of calcium nitrate ($Ca(NO_3)_2.4H_2O$; Merck), triethyl phosphite (TEP [$P(C_2H_5O)_3$]; Merck) and ammonium fluoride (NH_4F; Merck) were used. TEP was hydrolyzed in ethanol with a small amount of distilled water, then NH_4F was added to it and stirred vigorously for 24 h. In a separate container, a stoichiometric amount of calcium nitrate was dissolved in ethanol and vigorously stirred for 24 h. The Ca-containing solution was added slowly to the P-containing solution, and then aged at room temperature for 72 h and at 40 ºC for 24 h afterwards [5]. The composition ratios of [Ca]/[P], [OH]/[P] and [P]/[F] were kept at 1.67, 4 and 6, respectively.

The samples of cp-titanium were cut into sheets with the dimensions of 20 mm ×20 mm ×1 mm. The samples were washed with distilled water and sequentially polished with abrasive papers (400, 600, 800, 1000, 1200, 1500 and 2000 grit). They were cleaned in

Table 1. Average crystallite size of rutile and apatite phases in different temperatures.

Phase	Crystallite size (nm)		
	550 ºC	700 ºC	800 ºC
Rutile	-	52	307
Apatite	14	21	31

acetone and ethanol and finally kept in 400 ºC for 10 min. to remove organic agents.

The FHA films were prepared by dipping at a withdrawal speed of 3 cm/min. The obtained films were dried in an oven at 150 ºC for 10 min., and then heat treated at 550, 700 and 800 ºC. The deposition was repeated four times to increase the thickness of the films.

Phase compositions were estimated with X-ray diffraction (XRD- D4, Siemens, Bruker Co., Germany) with CuKα radiation (wavelength=1.54056 Å). The structural change was observed with fourier transform infrared (FT-IR, D4, SIEMENS, Bruker Co, Germany) analysis using KBr as a standard. The samples used in FT-IR studies were taken from the coatings. Scanning electron microscopy (SEM, Leo 440I, England) was used to study the thickness and morphology of deposited samples.

Finally, the crystallite size of the rutile and apatite phases were evaluated from the peak broadening of XRD patterns based on Scherrer's formula as follows [22]:

$$D = \frac{0.9\,\lambda}{FWHM.Cos\theta} \qquad (1)$$

in which D is the crystallite size (Å), λ is the wavelength of the monochromatic X-ray beam (λ=0.154056 nm for CuKα radiation), FWHM is the full width at half-maximum for the diffraction peak under consideration (rad), and θ is the diffraction angle (deg).

3. Results and discussion

XRD patterns of samples heat treated at different temperatures are presented in Figure 1. The characteristic peaks of apatite can be identified in the range of 2θ=25-35. The intensity of peaks and crystallinity increased with the temperature of heat treatment. XRD pattern of the sample heat treated in 550 ºC (Figure 1A) showed the coating composed of the FA and HA. In addition, rutile (TiO_2) phase formed in the samples heat treated at higher temperatures. The heat treatment at 800 ºC led to form more amount of rutile phase as compared to heat treatment at 700 ºC. The average crystallite size of rutile and apatite phases that estimated from the Scherrer formula are shown in Table 1.

Fourier Transform Infrared spectroscopy (FT-IR) spectra are shown in Figure 2. The

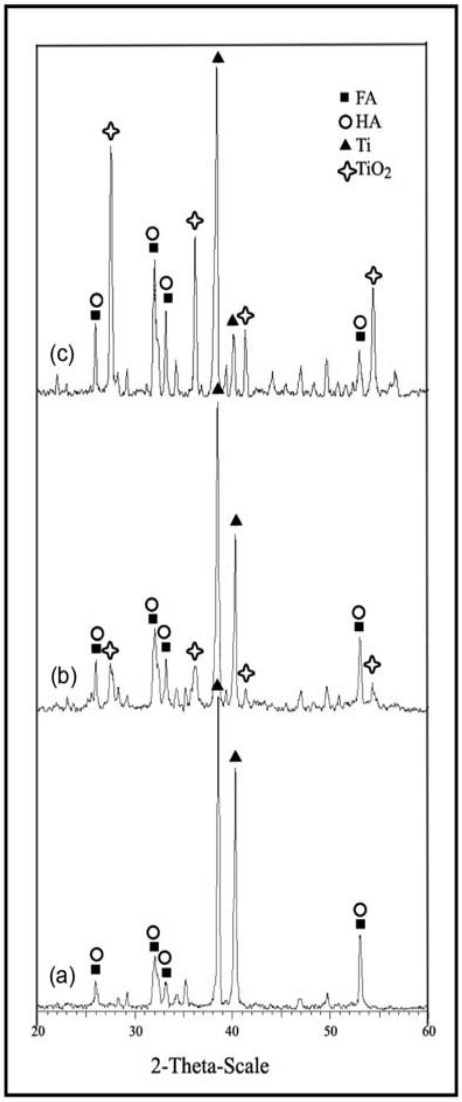

Figure 1. XRD patterns of the FHA-coated samples, heat treated at different temperatures; (a): 550 ºC; (b): 700 ºC; (c): 800 ºC.

typical characteristic P-O bands of apatite structure (550-610 and 950-1100 cm^{-1}) were identified in all samples. The peaks corresponding to OH group of apatite structure 632 cm^{-1} was appeared in all samples whereas it's other peak in 3500-3550 (3541) cm^{-1} due to hydrogenic bond with fluoride ions was only found in samples FHA700 and FHA800. The latter has not been reported by Kim *et al*. [10]. As reported by Rodrigo [23], the main difference between IR spectrum of HA and FA is the bond 3500-3650 cm-1. It should be noted that in the absence of F ions, the peak of OH-group in FHP (3541 cm^{-1}) appears in 3573 cm^{-1}.

The P-O peak in 964 cm^{-1} has been hidden in the broad P-O peak in 1044 cm^{-1} for the sample FHA400. The absence of P-O peak in 603 cm^{-1} for the sample FHA400, the sharpening of the peak in 1044 cm^{-1} for the sample FHA500 and the presence of P-O peaks in 400-500 cm^{-1} for the samples FHA700 and FHA800 would indicate an improvement in the atomic arrangement of the apatite structure.

In addition, the specified small peak in 866 cm^{-1} is related to the HPO_4^{2-} bond [24, 25]. It suggests the synthesized FHA could contain a calcium deficient hydroxyapatite (CDHA) which is confirmed by Ca/P ratio of 1.59 (sample FHA500) measured by ICP. The incorporation of the carbonate group is believed to be correlated to the non-stoichiometric nature of apatite structure [10].

In spite of the peak in 866 cm^{-1}, absorbing bond in 1360-1460 cm^{-1}, corresponding to

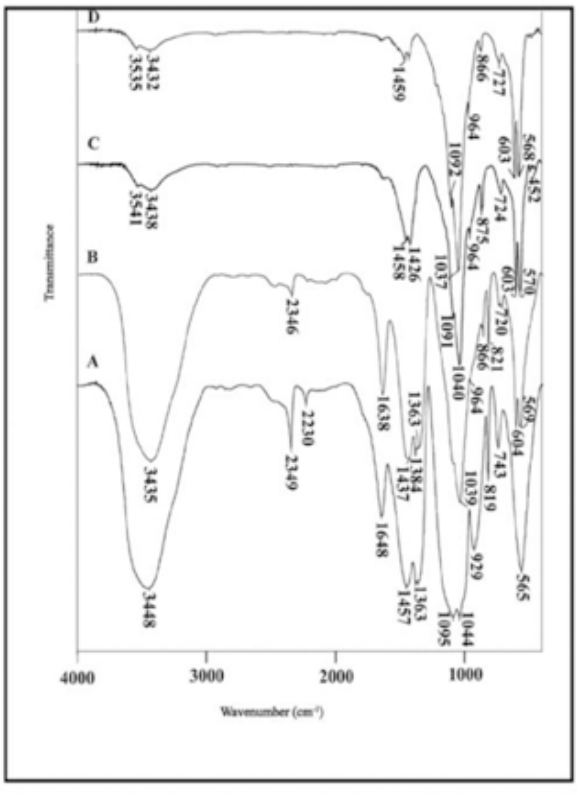

Figure 2. FT-IR spectra of the FHA-coated samples, heat treated at different temperatures; (a): 400 ºC; (b): 550 ºC; (c): 700 ºC; (d): 800 ºC.

the C-O bonds of the carbonate groups, decrease with the temperature. It confirms the sample FHA400 contained carbonate groups within the apatite structure to a higher degree. The peak intensity decrease and sharpening of the C-O bonds with the heat treatment temperature can be also attributed to the liberation of carbonate groups contained in a higher ordering of atomic structure.

The peak in 1648 cm^{-1} and the large peak in 3435 cm^{-1} corresponding to the bending modes of O-H bond of water decreased significantly with the increasing of temperatures. The bond of 821 cm^{-1} for the nitrate group in dried gel, disappeared gradually with the increasing of temperature.

Considering the SEM images taken from outer surface of coatings (Figure 3), the samples heat treated at 550 ºC and 700 ºC have almost the same morphology. As shown in Figure 3d and f, the coating of sample heat treated at 800 ºC composed of the nano-sized grains and porosity smaller than sample heat treated at 700 ºC. For the latter, it seems that the porosities are interconnected. In comparison with the other samples, it appears the coating of samples heat treated in 800 ºC

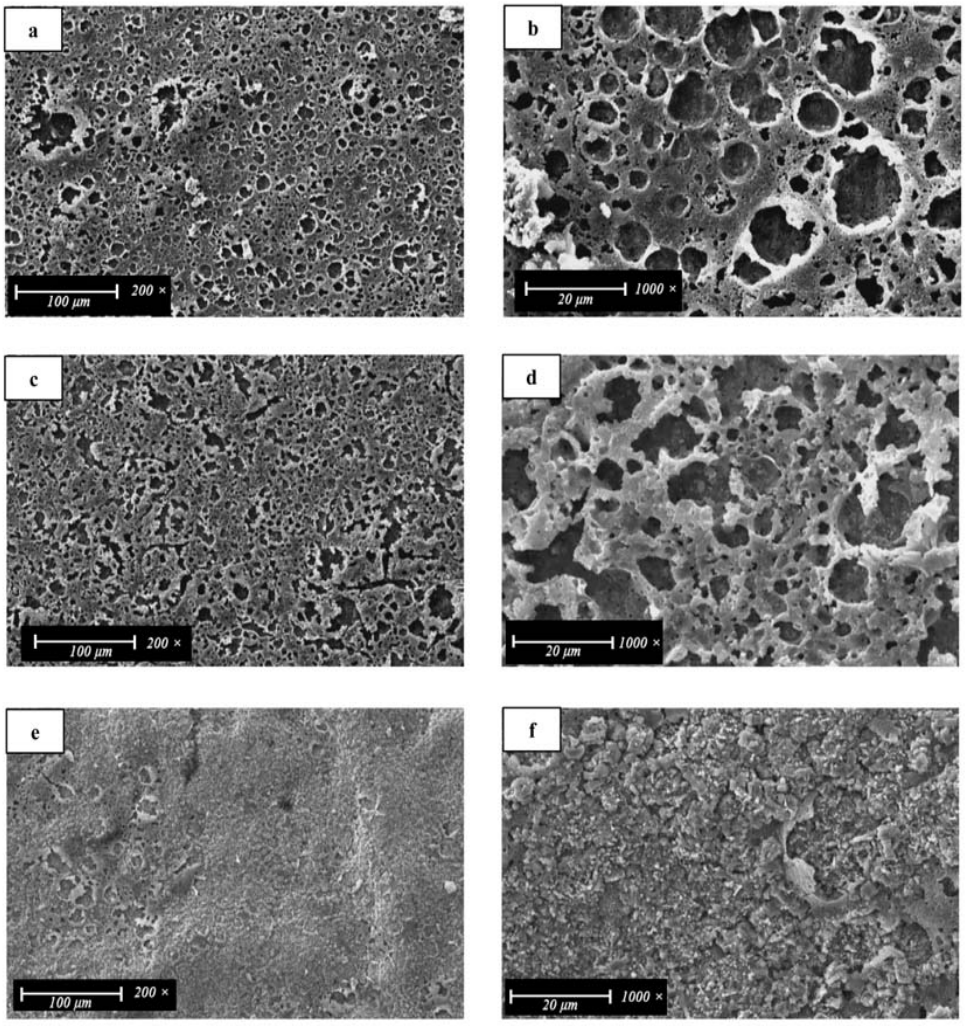

Figure 3. SEM images of the outer surfaces of FHA-coated samples, heat treated at different temperatures: (a, b): 550° C; (c, d): 700 ° C; (e, f): 800 °C.

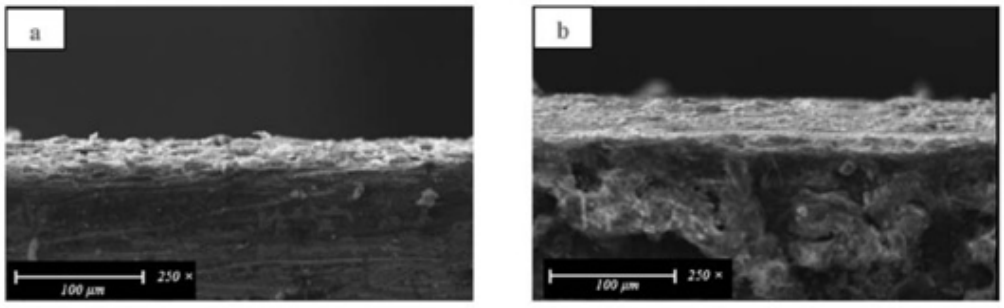

Figure 4. Cross sectional SEM images of the FHA-coated samples, heat treated at different temperatures; (a): 500 °C; (b): 700 °C.

was more homogenous and smooth and no considerable porosities can be observed. The crystalline grains are clearly visible in the image taken from the coating of this sample (Figure 3f). Figure 4a and b shows cross sectional images of samples heat treated at 550 ºC and 700 ºC.

4. Conclusion

Based on the results obtained in this work, HA and FA formed in all samples. Also, FT-IR results showed the presence of FHA in the samples heat treated at temperatures higher than 550 °C. Heating treatment above 700 °C resulted in the formation of rutile phase. The crystallinity and thicknesses of coating layers increased with rising heat treatment temperature. The coating heat treated at 800 °C was very homogenous and crystalline without any trace of porosity.

5. Acknowledgments

The authors thanks the specialists and the several laboratories of Materials and Energy Research Center and X-ray diffraction lab of Geology and Mineral Discovery Institute, the laboratory complex center of Islamic Azad university (science and research branch) for their precious cooperation and comments. Finally, they appreciate the financial support of the Iranian Nanotechnology Initiative.

References

[1] De Lange GL, Donath K. Interface between bone tissue and implants of solid hydroxyapatite or hydroxyapatite-coated titanium implants. *Biomaterials* 1989; 10: 121-5.

[2] Hench LL. Bioceramics: From concept to clinic. *J Am Ceram Soc* 1991; 74: 1485-510.

[3] Overgaard S, Soballe K, Hansen ES, Josephsen K, Bunger C. Implant loading accelerates resorption of hydroxyapatite coating. *J Orthop Res* 1996; 14: 888-94.

[4] Bloebaum RD, Dupont JA. Osteolysis from a press-fit hydroxyapatite-coated implant. A case study. *J Arthroplasty* 1993; 8: 195-202.

[5] Kim HW, Kong YM, Bae CJ, Noh YJ, Kim HE. Sol-gel derived fluor-hydroxyapatite biocoatings on zirconia substrate. *Biomaterials* 2004; 25: 2919-26.

[6] Okazaki M, Miake Y, Tohda H, Yanagisawa T, Takahashi J. Differences in solubility of two types of heterogeneous fluoridated hydroxyapatites. *Biomaterials* 1998; 19: 611-6.

[7] Larsen MJ, Jensen SJ. Solubility, unit cell dimensions and crystallinity of fluoridated human dental enamel. *Arch Oral Biol* 1989; 34: 969-73.

[8] Moreno EC, Kresak M, Zahradnik RT. Fluoridated hydroxyapatite solubility and caries formation. *Nature (London)* 1974; 247: 64-5.

[9] Kim HW, Kim HE, Knowles JC. Fluor-hydroxyapatite sol-gel coating on titanium substrate for hard tissue implants. *Biomaterials* 2004; 25: 3351-8.

[10] Kim HW, Li LH, Koh YH, Knowles JC, Kim HE. Sol-gel preparation and properties of fluoride-substituted hydroxyapatite powders. *J Am Ceram Soc* 2004; 87; 1939-44.

[11] Gross KA, Rodriguez-Lorenzo LM. Sintered fluorhydroxyapatites. Part 1: Sintering ability of precipitated solid solution powders. *Biomaterials* 2004; 25: 1375-84.

[12] Marie PJ, Hott M. Short term effects of fluoride

and strontium on bone formation and resorption in the mouse. *Metabolism* 1986; 35: 547-51.

[13] Elliott JC. *Structure and chemistry of the apatites and other calcium orthophosphates*. Elsevier Science; The Netherlands; 1994; p. 4.

[14] Aoba T. The effect of fluoride on apatite structure and growth. *Crit Rev Oral Biol Med* 1997; 8: 136-53.

[15] Cheng K, Han G, Weng W, Qu H, Du P, Shen G, Yang J, Ferreira JMF. Sol-gel derived fluoridated hydroxyapatite films. *Mate Res Bulletin* 2003; 38: 89-97.

[16] Kay JF. Calcium phosphate coatings for dental implants: Current status and futur potential *Dent Clin North Am* 1992; 36: 1-18.

[17] Ducheyne P, Cuckler JM. Bioactive ceramic prosthetic coatings. *Clin Orthop Relat Res* 1992; 276: 102-14.

[18] Cheang P, Khor KA. Addressing processing problems associated with plasma spraying of hydroxyapatite coatings. *Biomaterials* 1996; 17: 537-44.

[19] Kim HW, Knowles JC, Kim HE. Hard tissue engineered hydroxyapatite coatings on zirconia porous scaffold by sol-gel and slurry method. *J Biomed Mater Res* 2004; 70B: 270-7.

[20] Kim HW, Koh YH, Li LH, Kim HE. Hydroxyapatite coatings on titanium substrate with titania buffer layer processed by sol-gel method. *Biomaterials* 2004; 25: 2533-8.

[21] Liu DM, Yang Q, Troczynski T. Sol-gel hydroxyapatite coatings on stainless steel substrates. *Biomaterials* 2002; 23: 691-8.

[22] Cullity BD. *Elements of X-ray diffraction*. 2nd ed. Massachuset: Addison-Wesley Publishing, 1978.

[23] Rodrigo CP. Synthesis and characterization of strontium fluorapatite. Bachelor of Science Thesis, University of Colombo, Sri Lanka, 2001.

[24] Emerson WH, Fischer EE. The infra-red absorbtion spectra of carbonate in calcified tissues, *Arch Oral Biol* 1962; 7: 671-83.

[25] Elliott JC, Holcomb DW, Young RA. Infra-red determination of the degree of substituation of hydroxyl by carbonate in human dental enamel *Calcif Tissue Int* 1985; 37: 372-5.